Cell, Vol. 99, 463–472, November 24, 1999, Copyright ©1999 by Cell Press

An Auxin-Dependent Distal Organizer of Pattern and Polarity in the *Arabidopsis* Root

Sabrina Sabatini,[1,7] Dimitris Beis,[1,7] Harald Wolkenfelt,[1] Jane Murfett,[2] Tom Guilfoyle,[2] Jocelyn Malamy,[3] Philip Benfey,[3] Ottoline Leyser,[4] Nicole Bechtold,[5] Peter Weisbeek,[1] and Ben Scheres,[1,6]
[1]Department of Molecular Cell Biology
Utrecht University
Padualaan 8
3584 CH Utrecht
The Netherlands
[2]Department of Biochemistry
University of Missouri
Columbia, Missouri 65211
[3]Biology Department
New York University
New York, New York 10003
[4]Department of Biology
University of York
York YO10 5YW
United Kingdom
[5]Laboratoire de Genetique et Amelioration des Plantes
INRA-Centre de Versailles
France

Summary

Root formation in plants involves the continuous interpretation of positional cues. Physiological studies have linked root formation to auxins. An auxin response element displays a maximum in the *Arabidopsis* root and we investigate its developmental significance. Auxin response mutants reduce the maximum or its perception, and interfere with distal root patterning. Polar auxin transport mutants affect its localization and distal pattern. Polar auxin transport inhibitors cause dramatic relocalization of the maximum, and associated changes in pattern and polarity. Auxin application and laser ablations correlate root pattern with a maximum adjacent to the vascular bundle. Our data indicate that an auxin maximum at a vascular boundary establishes a distal organizer in the root.

Introduction

The organization of pattern and polarity by asymmetrically distributed molecules is a recurring theme in development. In animals, such molecules may be laid down in the egg, they may be induced by external cues, or their distribution may result from the interaction between cell groups at their boundaries (e.g., Ingham and Martinez Arias, 1992; St. Johnston and Nusslein-Volhard, 1992). In all cases, the distribution of the organizing molecule is necessary and sufficient to instruct cell fate decisions in responsive cells.

[6] To whom correspondence should be addressed (e-mail: b.scheres@bio.uu.nl).
[7] These authors have contributed equally to this work and should be considered joint first authors.

Plants contain many different cell types in ordered spatial patterns. Pattern formation initiates in the embryo and is elaborated in the meristems, foci of continuous development (Steeves and Sussex, 1989). The multicellular state has evolved independently in the plant kingdom, but molecular genetic studies have uncovered mechanisms similar to those operating in animal development. For example, receptor–ligand interactions control the decision of cells to differentiate in shoot and floral meristems (Clark et al., 1997; Fletcher et al., 1999) and a combinatorial code of transcription factors specifies floral organ identity (Parcy et al., 1998). Nevertheless, it is still unclear how meristems organize spatial patterns of cell differentiation.

Auxins such as indole-3-acetic acid (IAA) are classical plant hormones that influence cell division, cell elongation, cell differentiation and the initiation of organ formation (Davies, 1995). Interference with auxin transport in the embryo leads to embryonic pattern aberrations (Liu et al., 1993; Hadfi et al., 1998). Auxins may also affect cell type choice, as suggested by their capacity to induce vascular strand formation (Sachs, 1991; Mattsson et al., 1999). Genetic studies have strengthened the notion that auxins play a role in pattern formation. For example, the *MONOPTEROS* (*MP*) gene is essential for the specification of basal regions in the embryo and for the formation of continuous vascular strands (Berleth and Jurgens, 1993). The MP protein is strikingly similar to AUXIN RESPONSE FACTOR 1 (ARF1), a transcription factor that binds auxin-responsive promoter elements, and is thought to mediate responses to auxins (Ulmasov et al., 1997a; Hardtke and Berleth, 1998). Mutations in the *Arabidopsis ETTIN* (*ETT*) gene suggest that it is required for the positioning of different gynoecium regions. The ETT protein contains a DNA-binding domain similar to that of ARFs (Sessions et al., 1997). Thus, auxins are correlated with patterning processes, and one can question whether asymmetrically distributed auxin provides patterning information. A test of this hypothesis requires the visualization of auxin distribution and possibilities to modulate this distribution and its perception.

Auxins act in the micro- to nanomolar range and their exact cellular distribution is not known, although steep concentration gradients have been observed (Uggla et al., 1996). Asymmetric auxin distributions can arise from selective production and degradation, but also from regulated auxin transport. Polar auxin transport has been measured in many classical assays and specific inhibitors are available (Davies, 1995). Components of transporters, asymmetrically located in membranes of specific cell types, have now been identified and the observed locations are consistent with prevailing models of auxin transport (Bennett et al., 1996; Chen et al., 1998; Galweiler et al., 1998; Luschnig et al., 1998; Muller et al., 1998).

Although the signal transduction pathway from auxin perception to response is not yet clarified, a set of gene products have been shown to interact with the ARF family of transcription factors, determining sensitivity and possibly output (Kim et al., 1997; Ulmasov et al.,

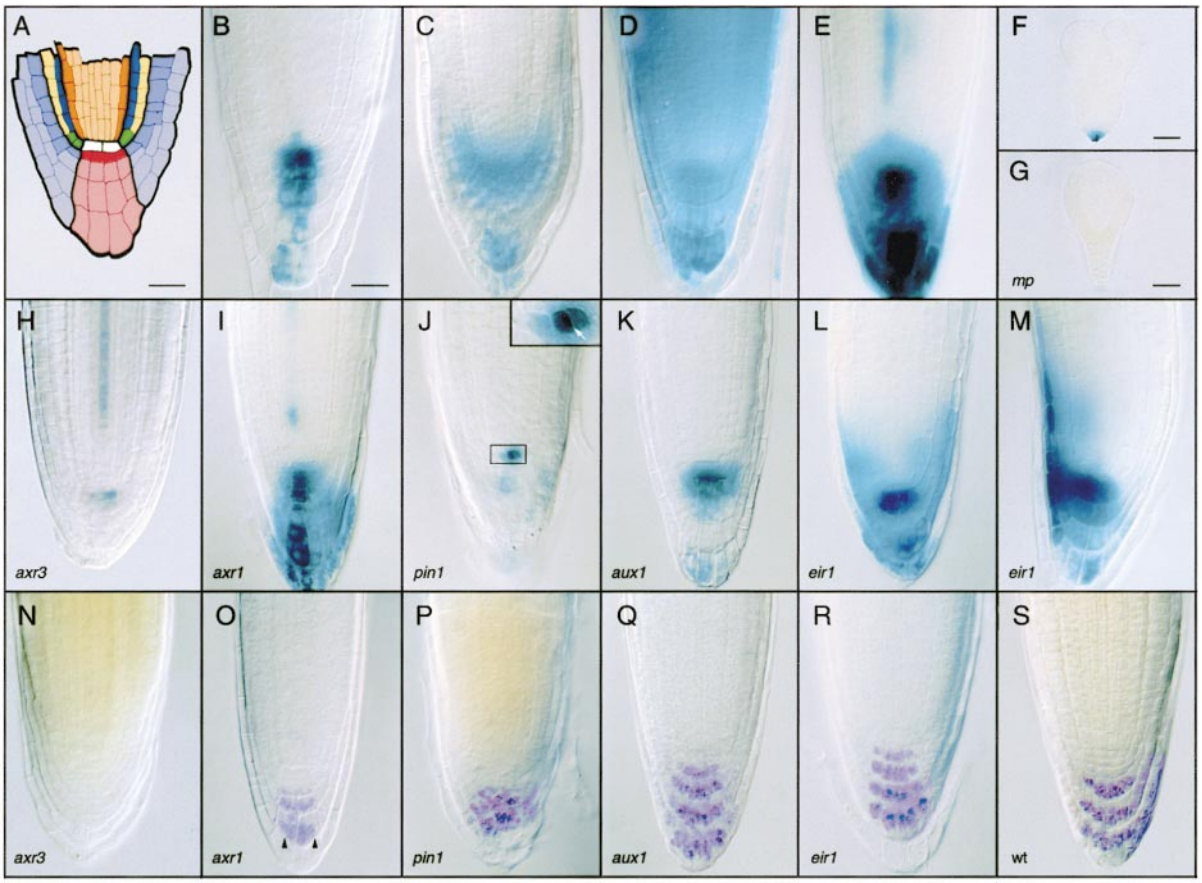

Figure 1. The DR5 Auxin Reporter Maximum in the *Arabidopsis* Root Is Modulated by Auxin Response and Auxin Transport Mutants

(A) Organization of the *Arabidopsis* root meristem, median longitudinal view. Single layers of epidermis (purple), cortex (yellow), endodermis (blue) surround the vascular bundle (orange) with the pericycle (dark orange) at its boundary. Lateral root cap (light purple), columella root cap (pink), and quiescent center (white) are distal-specific cell types. All initials (stem cells) surround the quiescent center; the cortical/endodermal initials are marked in green and the columella initials in red.

(B and E) An expression maximum of DR5::GUS reporter homozygotes (*DR5/DR5*) in columella initials of 4 dpg seedlings. (B) 30′ staining; (E) 16 hr staining.

(C) Expansion of the DR5::GUS expression maximum in 4 dpg seedlings on medium containing 10 μM NPA.

(D) All cells are able to switch on DR5::GUS expression upon 2,4D application.

(F) An expression maximum of the DR5::GUS reporter in prospective columella cells of a heart stage embryo. 16 hr staining.

(G) No DR5::GUS expression in a mp^{u21}/mp^{u21}, *DR5/DR5* embryo after 16 hr staining.

(H–M) DR5::GUS expression in 4 dpg auxin response and transport mutants. (H–I) 16 hr staining. (H) *axr3-1/+*, *DR5/DR5*. (I) *axr1-12/axr1-12, DR5/DR5*. (J–M) 30 min staining. (J) *pin1-1/pin1-1, DR5/DR5* (arrow in inset points to the aberrant cell division of the QC). (K) *aux1-7/aux1-7, DR5/DR5*. (L–M) *eir1-1/eir1-1, DR5/DR5*. (L) gravity vector aligned with proximodistal axis. (M) gravity vector not aligned.

(N–R) Columella specification visualized by starch granule staining in the same genotypes depicted in (H–L). Arrowheads in (O) point to the two columella columns in *axr1-12* homozygotes.

(S) Starch granule staining in wild type.

DIC optics of cleared root tips and embryos. Bars, 25 μm.

1997b; Rouse et al., 1998; Tian and Reed, 1999). Furthermore, the ubiquitination pathway has been shown to play a role in auxin sensitivity, possibly by regulating proteolysis of short-lived repressors (Leyser et al., 1993; Ruegger et al., 1998).

The possibility to modulate auxin distribution and response using the genetic tools described above now allows direct tests of the role of auxin in patterning. We have utilized the *Arabidopsis* root meristem, where strict lineage relationships facilitate analysis (Dolan et al., 1993; Scheres et al., 1994). We use a reporter construct with ARF-binding *cis*-elements to visualize free auxin and find a maximum in the distal region of the root meristem. Mutants defective in auxin transport and response indicate that generation of this maximum and its perception are necessary for correct patterning. Ectopic auxin accumulation, induced by three different methods, is sufficient for dramatic repatterning and the position of a new maximum relative to vascular cells determines the pattern of distal cell types as well as cell and tissue polarity. We conclude that asymmetric auxin distribution establishes an organizer of pattern and polarity in the root meristem.

Results

A Distal Auxin Maximum in the *Arabidopsis* Root

The *Arabidopsis* root has an uncomplicated radial organization (Figure 1A). From outside to inside, concentric

layers of epidermis, cortex, and endodermis encircle the stele that contains the vascular system. New cells are added to extend the radial pattern of mature cells in the zone of mitotic activity, the meristem. The basal-most cells in these files, termed initials, are stem cells. Four quiescent center (QC) cells contact all initials and they are required to maintain their stem cell status (van den Berg et al., 1997). The columella initial cells and the epidermal initials give rise to the columella and lateral root cap, respectively, of which the outermost cells detach from the root.

In order to visualize auxin distribution, we used a fusion of a synthetic promoter consisting of 7 tandem repeats of an auxin-responsive TGTCTC element and a minimal 35S CaMV promoter with the β-glucuronidase (GUS) reporter gene, hereafter called DR5::GUS (Ulmasov et al., 1997b). The TGTCTC element resides in many early auxin response genes, binds ARFs, responds rapidly to active auxins only, increases its response between 10^{-8} and 10^{-5} M and remains at high levels up to 10^{-4} M (Ulmasov et al., 1997a, 1997b; T. G., unpublished). We reasoned that a small synthetic promoter with this element was the best available tool to visualize responses to active auxins at cellular resolution. DR5::GUS plants displayed a maximum of GUS activity in the columella initial cells, with lower activity in the QC and mature columella root cap (Figure 1B). Inhibition of polar auxin transport with 1-N-naphthylphthalamic acid (NPA) (Figure 1C) and the unrelated compound 2,3,5-triiodobenzoic acid (TIBA) (data not shown) shifted and expanded the maximum in DR5::GUS plants, showing that the localization of DR5 activity was dependent on auxin transport. Addition of the auxin 2,4-dichlorophenoxy acetic acid (2,4-D) resulted in staining of all cells of the root (Figure 1D). Importantly, QC and columella cells did not display elevated sensitivity to externally applied auxin. Thus, within the root meristem, DR5 activity monitored auxin levels in a cell type–independent manner and did not reflect spatial differences in auxin sensitivity.

We quantified GUS activity in isolated root tips and mature roots. Approximately 3.5-fold higher levels of DR5 activity were detected in the tip compared to mature roots, and NPA addition led to a further ~3-fold increase only in the tips. Free auxin levels have been measured by tandem mass spectrometry in adjacent regions of the *Arabidopsis* root; the highest levels were detected in the distal tip region, and NPA treatment led to an increase that was most dramatic in the distal tip region (G. Sandberg, personal communication). These measurements correlate well with DR5::GUS activity in untreated and NPA-treated plants, consistent with the notion that DR5 activity monitored high levels of free auxin in the distal tip.

Mutants in Auxin Response Have Distal Patterning Defects

To evaluate the significance of the auxin response maximum in the distal root tip, we introduced the DR5::GUS reporter into mutants defective in auxin responses, and analyzed DR5 expression and formation of pattern elements in the root.

Recessive mutations in the *MP* gene, encoding an ARF-type transcription factor capable of binding auxin response elements (Ulmasov et al., 1997a, 1999), completely abolish embryonic root formation and distal root pattern elements are absent (Berleth and Jurgens, 1993; Hardtke and Berleth, 1998). In wild-type embryos, a DR5 peak occurred in the future root region at the heart stage, well before the onset of root meristem activity and the differentiation of columella cells (Figure 1F). No DR5 expression was detected in the basal end of strong mp^{U21} mutant seedlings and embryos at any stage (Figure 1G). We were able to induce high expression by external auxins (data not shown), and thus the DR5 maximum does not directly depend on the MP transcriptional regulator. Consistent with these findings, it has been suggested that reduced auxin sensitivity in *mp* mutants affects auxin transport in the embryo, indirectly leading to patterning defects (Mattsson et al., 1999).

The *AXR1* gene encodes a protein with overall homology to yeast ENR2, involved in protein degradation by conjugation of the ubiquitin-like protein Rub1p (Leyser et al., 1993; Walker and Estelle, 1998). *axr1* mutants show reduced auxin responses. DR5 expression was reduced in *axr1* mutants but its spatial distribution was unaltered (Figure 1I, compare with 1E). In ~50% of seedlings homozygous for the strong *axr1-12* allele, and ~25% of seedlings homozygous for the weak *axr1-3* allele, a reduction in the number of columella root cap columns was observed (Figure 1O, compare with 1S). The number of columns is established by stereotyped cell divisions in the progenitor cell of the columella. Thus, a reduction in DR5 activity due to reduced AXR1 activity is correlated with an incomplete cell division program in the distal root cap.

The *AXR3* gene encodes a protein that can interact with ARFs, and it has been implicated in auxin responses (Rouse et al., 1998). Dominant *axr3* mutations are thought to cause a greater stability of the protein. The resulting auxin responses are in some cases enhanced and in other cases reduced. DR5 activity in the distal primary root was dramatically reduced in *axr3-1* mutant background (Figure 1H, compare with 1E). Correlated with this reduction, columella cells were not appropriately specified in *axr3-1* mutants. Starch granules did not form (Figure 1N), and we never observed newly divided columella initial cells indicating that these are inactive. Thus, *axr3-1* interferes with the establishment of the DR5 maximum in the primary root and with the acquisition of the associated cell fates.

In conclusion, three unrelated auxin response mutants show a decrease in DR5 activity and correlated defects in cell fate or patterned cell division. Although the primary roles and the specificity of the corresponding genes in auxin signaling remains to be established, this correlation indicates that the perception of an auxin peak in the distal root tip is required for the correct specification of distal pattern elements and cell division programs.

Mutants in Auxin Transport Have Distal Patterning Defects

Although local synthesis and inactivation can affect auxin distribution, it is attractive to hypothesize that recently identified auxin transporters mediate auxin distribution. The *AtPIN1* and *EIR1* (also referred to as *AtPIN2/AGR1/WAV6*) genes encode transmembrane proteins capable of mediating cellular efflux of auxin. PIN1 is

localized at the basal membranes of xylem parenchyma cells, whereas EIR1 is localized at the apical membrane of epidermal cells and at a subset of cortical cell membranes (Galweiler et al., 1998; Muller et al., 1998). The *AUX1* gene, encoding a transmembrane protein with homology to bacterial permeases, mediates auxin influx and is expressed predominantly in the lateral root cap and epidermis of the root meristem (Marchant et al., 1999). We tested whether the correct localization of the DR5 maximum required the *AtPIN1, EIR1*, and *AUX1* genes, and we analyzed the effects of mislocalization on pattern formation.

The spatial distribution of DR5 expression was affected in ~30% of *pin1-1* mutants. An overall reduction in DR5 levels was frequently accompanied by ectopic DR5 peak levels in unusual positions like in the QC (Figure 1J). Ectopic expression was associated with changes in otherwise strictly oriented cell divisions (Figure 1J, inset), and with a distorted organization of the columella (Figure 1P). In *eir1-1* background, ectopic accumulation of DR5 activity was observed in the lateral root cap (Figure 1L). If the growth direction of *eir1* seedlings was not manually aligned to the gravity vector, prominent DR5 accumulation occurred on one side of the lateral root cap, consistent with a defect in lateral transport of auxin upon gravitropic stimulation (Figure 1M). The root tips of these seedlings displayed a characteristic curvature related to the lateral root cap maximum, suggesting a cell elongation response to lateral auxin accumulation (Figure 1M). No changes in cell specification were observed. Neither DR5 distribution, nor the distal root pattern was changed in the *aux1-7* mutant (Figures 1K and 1Q).

We concluded that the AtPIN1 and EIR1 efflux carrier components, but not AUX1, are required for the correct localization of the DR5 peak. Mutations in the individual efflux components, however, did not entirely mislocalize the DR5 peak, which is consistent with the mild patterning defects that were observed. Defective cell division patterns in *pin1* suggest that the exact localization of auxin is required for the oriented cell divisions that accompany pattern formation, and differences in cell elongation in *eir1* suggest that the exact localization of auxin influences cell elongation.

Both *pin1* and *eir1* mutants uncouple the DR5 maximum from columella initial- and other cell fates associated with high DR5 levels, demonstrating that the cellular localization of the DR5 peak is not caused by prior cell type specification or vice versa. This observation is significant in two ways. First, the consistent correlation of DR5 levels and cell fates in the auxin sensitivity mutants discussed in the previous paragraph is meaningful only if these variables are separable. Second, the uncoupling of auxin levels and cell type indicates that distal patterning does not simply occur by cell-autonomous specification in relation to a particular auxin level.

Inhibition of Polar Auxin Transport Redirects Distal Pattern and Polarity

The observed correlation between a distal auxin maximum and distal pattern elements prompted us to investigate whether high auxin levels in the *Arabidopsis* root meristem are sufficient to direct the specification of cell fates and cell division planes. We sought to induce different auxin distributions and record changes in cell fate and cell division. As auxin transport mutants displayed only limited changes in DR5 distribution, we utilized specific polar transport inhibitors to establish more significant changes (Rubery, 1990). Dramatic changes in DR5 distribution were observed in roots germinated on NPA (Figures 2A, 2G, and 2M), and cell fates as well as the orientation and extent of cell division were strongly affected.

Several controls were performed to ascertain that cell fates changed due to a different auxin distribution. First, similar results were obtained with independent markers, verifying that marker gene changes visualized cell fate changes (see Experimental Procedures). Second, the polar transport inhibitor TIBA invoked the same responses, confirming that the changes are not specific to NPA (data not shown). Third, *axr1-12* and *axr3-1* mutants showed a strong reduction of these responses to NPA, which suggests that the inhibitor effects require auxin perception (data not shown).

In roots of 7 days postgermination (dpg) seedlings on 10 μM NPA, the DR5 peak occupied a cup-shaped domain, encompassing the original peak in the columella initials, but newly incorporating the flanking epidermal cells and, more proximal, cortical cells (Figures 2A and 2G). All these cells have in common their location two cell layers outside of pericycle/provascular cells (Figure 2G). Concomitantly with the shift in DR5 activity, the lateral cells divided in new planes perpendicular to the location of the pericycle/vascular bundle (Figure 2, arrowhead in G, inset in I, schematic in H). The dividing cells expressed the columella initial-specific enhancer trap J2341 (data not shown). They were flanked on the outside by cells expressing columella markers (Figures 2C and 2I), and on the inside by cells expressing QC-specific markers (Figures 2D and 2J). Not only did marker gene expression domains change, the cells in which these markers were expressed acquired the appropriate functional characteristics: (1) new columella cell layers were formed by the cells with columella initial markers; (2) these initials produced multiple layers, which reveals the QC-specific stem cell maintenance activity of the contacting cells with QC markers (van den Berg et al., 1997). We concluded that a lateral shift of the DR5 maximum correlates with the acquisition of QC, columella initial and differentiated columella identity of former epidermal, endodermal, and cortical cells.

The cortex daughter marker CD92 and the lateral root cap marker LRC244 (Malamy and Benfey, 1997a) visualize specific differentiation stages of cells in the proximal root meristem (Figures 2E and 2F). These markers regressed proximally and remained at a fixed distance of the expanding auxin maximum (Figures 2K and 2L), suggesting that the differentiation status of these tissues responds to the proximity of the maximum.

A Centralized Cylindrical Auxin Perception Maximum Results in Mirror-Image Duplication

The upward shift of the DR5 peak terminates at the proximal lateral root cap boundary (Figures 2R and 3F), and we were interested to determine the long-term effects of this distribution. Four weeks after germination

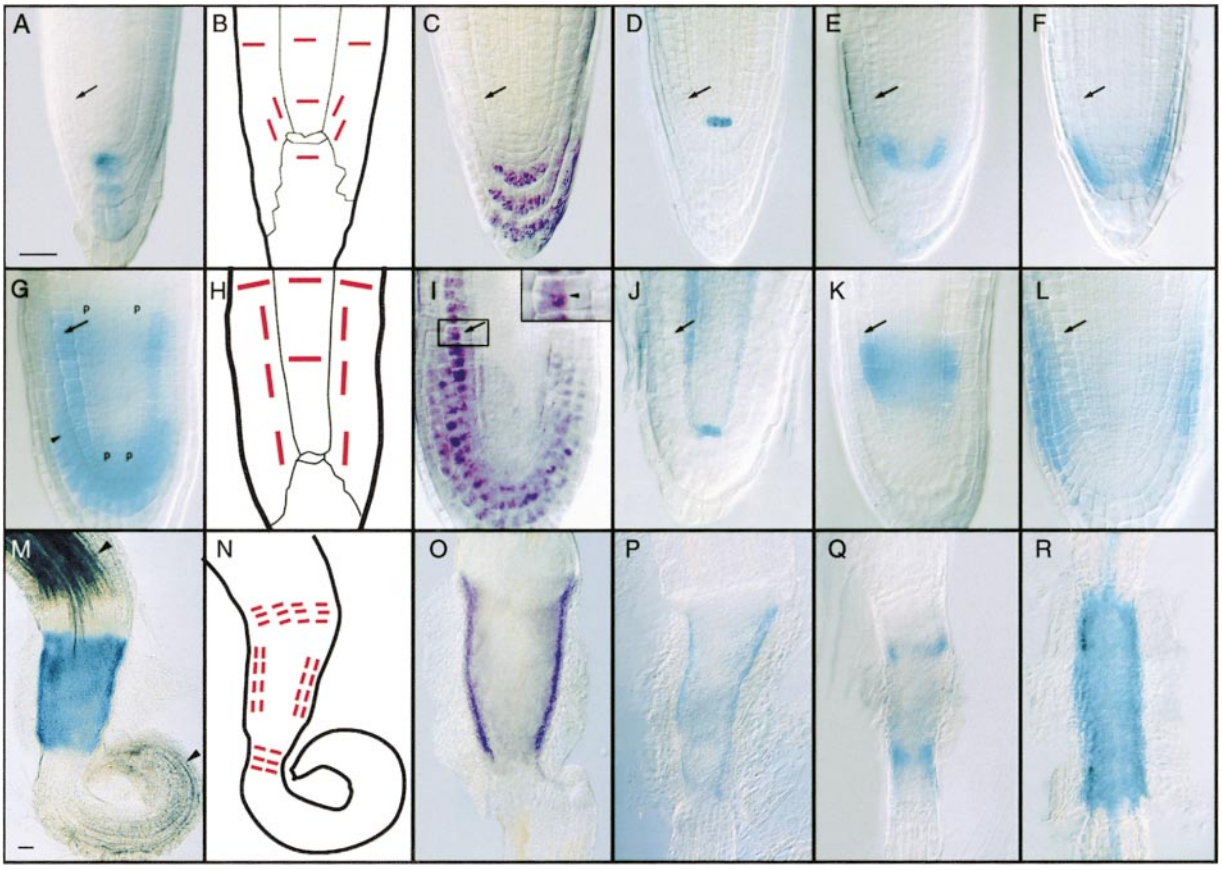

Figure 2. Inhibition of Polar Auxin Transport Shifts the DR5 Maximum and Redirects Distal Pattern and Polarity

(A–F) 4 dpg seedlings on medium without NPA.

(G–L) 7 dpg seedlings germinated on medium containing 10 μm NPA.

(M–R) Mirror-image duplicated roots in 28 dpg plants germinated on medium containing 50 μm NPA. A central zone with distal properties is flanked by two regions of intense cell division.

(A, G, and M) *DR5/DR5*, 30 min staining. (G) p indicates provascular/pericycle cells; arrowhead: aberrant periclinal division of the former epidermis. (M) arrowhead: xylem strands.

(B, H, and N) Schematic outlines of the *DR5/DR5* root tips. Regions of cell division and orientation of new cell walls in red.

(C, I, and O) Starch granule staining (arrowhead in [I] inset, points to a former cortex cell that contains high DR5::GUS activity and it has divided, producing an inner columella initial cell and an outer starch granule-containing columella cell).

(D, J, and P) GUS staining in a line heterozygous for the quiescent center–specific promoter trap QC46.

(E, K, and Q) GUS staining in a line heterozygous for the CD92 promoter trap, specific for the daughter cells of the cortex initials.

(F, L, and R) GUS staining in a line heterozygous for the lateral root cap–specific promoter trap LRC244.

Arrows indicate the position of the left cortex cell file.

DIC optics of cleared roots. Bars, 25 μm.

on 50 μM NPA, the upward shift was complete. The basally located original DR5 peak disappeared for reasons that we do not yet understand. The result was an open-ended, cylindrical DR5 peak in the former cortex, which resided at the center of a mirror-image duplicated root (Figures 2M–2R and 3). We will describe features of this central DR5-expressing region, and subsequently turn to its flanking proximal and distal regions.

Surrounding the cylinder with the DR5 maximum, a single layer of columella root cap initials (Figures 3A–3E, arrows) divided periclinally to create columella root cap layers on its outer side (Figures 2O and 3C). These layers, originating from the former cortex, were surrounded by lateral root cap layers originating from the former epidermis, with the original lateral root cap layer on the outermost side (Figures 2R, 3E, and 3F). To the inside of the DR5-expressing cylinder there was a single layer of cells expressing QC markers. This layer originated from the former endodermis (Figures 2P and 3B), which surrounded provascular tissue in which cells now divided periclinally as judged from the increase in the number of cell files. Not only the direction of vascular cell division was changed, but also the main axis of peripheral vascular cells became reoriented toward the DR5 maximum (Figure 3I, arrow). We concluded that an auxin maximum with cylindrical shape is correlated with the formation of single cell layers of QC and columella initial identity, flanked by differentiated columella and lateral root cap. These layers surround provascular cells in which the orientation of cell division and of cell expansion adapts to a new axis of tissue polarity.

In the distal and proximal regions surrounding the

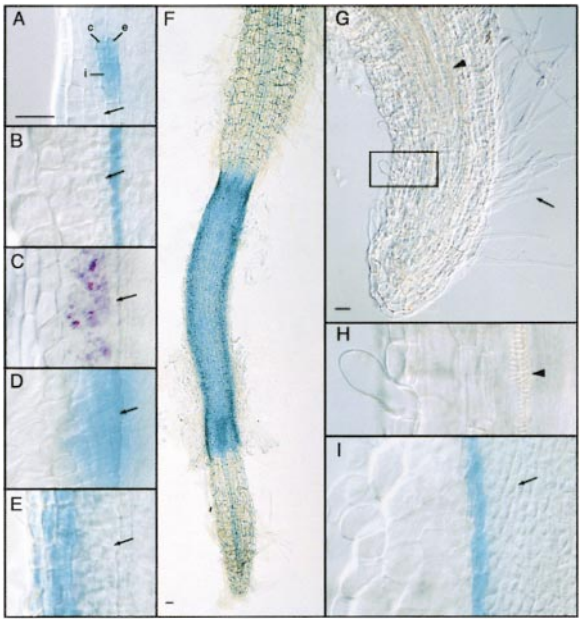

Figure 3. NPA-Induced Mirror-Image Duplications Contain a Central Region with Precisely Patterned Distal Cell Types and Active Proximal and Distal Meristems

(A–E) The central region of a 28 dpg seedling contains concentric rings of distal cell types, flanked on both sides by meristematic initial cells (arrows point to columella initials). (A) Proximal boundary of the central region. Expression of CD92 highlights the position of the cortical initial. (B) A single layer of QC46-expressing cells in the former endodermis to the inside of the DR5 maximum. (C) Starch granule staining; concentric columella layers originating from the inner layer of the former cortex. (D) The DR5 maximum in the inner layer of the former cortex. (E) The LRC244 promoter trap highlights lateral root cap layers that originate from the epidermis. The outer layer is already formed prior to NPA treatment.

(F) The outermost lateral root cap layer visualized by the LRC244 promoter trap marks the proximal and distal boundary of the root meristem prior to NPA treatment.

(G) Distal-most region of duplicated root. The distal meristem produces cells that progressively differentiate from proximal to distal. Arrow: root hairs with inverted polarity. Arrowhead: xylem vessel.

(H) Blow-up of (G) showing a root hair that emerges from the apical end of an epidermal cell and a differentiated xylem vessel (arrowhead).

(I) GUS staining in a line heterozygous for the quiescent center–specific promoter trap QC46. Peripheral provascular cells at the proximal edge of the central region reorient their main axis toward the periphery (arrow).

DIC optics of cleared roots; Bars, 25 μm.

DR5-expressing cylinder, rings of expression marked cortical daughter cells (Figure 2Q) adjacent to new initial cells for cortex and endodermis (Figure 3A). This expression pattern suggests that two sets of initial (stem) cells arise distally and proximally of the DR5-expressing cylinder. Indeed, two flanking regions of cell division (i.e., meristems), and accompanying elongation and differentiation zones, now extended two root ends (Figures 3F–3H). The two root systems have an opposite polarity, as judged from the relative location of the zones of cell division, cell elongation (Figures 2M–2R), and cell differentiation (Figure 3G). The broadened vascular cylinder, which has been described previously in connection with auxin transport inhibition (Mattsson et al., 1999), contained multiple xylem strands in both differentiation zones (Figures 2M and 3G). Moreover, epidermal cell polarity in the basal root was reversed as indicated by root hairs growing in the opposite direction and originating from apical instead of from basal cell ends (Figures 3G and 3H).

Respecification of distal cell fate in defined cell layers, and reorientation of cell divisions in specific planes, are major aspects of the late response but they occur already within 1 day after transferring untreated seedlings to NPA (data not shown). Thus, these aspects of the late response appear to arise by spatial expansion of an early response without qualitative changes.

We concluded that ectopic auxin accumulation resulting from transport inhibition in the root meristem is sufficient to organize patterned distal cell fates and orientation/extent of cell division. The position of the maximum also correlates with organ and cell polarity.

The Location of an Auxin Maximum Relative to the Vascular Bundle Predicts Pattern and Polarity

The changes following the inhibition of polar auxin transport suggest that an auxin-induced organizer is capable of specifying distal pattern and polarity, but they do not reveal which additional positional cues are required. In the simplest interpretation, auxin concentration differences alone could specify pattern and polarity. This model predicts that different cellular DR5 distributions correlate exactly with cell types. This prediction cannot be easily reconciled with our earlier finding that auxin peak levels can be separated from cell type, but we wanted to test it independently by exogenous addition of auxins to *DR5::GUS* plants. The synthetic auxin 2,4D, which is not redistributed by export carriers (Delbarre et al., 1996), induced the largest DR5::GUS activity in the outer epidermal layer and less in the inner layers (Figure 4D).

Ectopic DR5::GUS activity upon 2,4D addition was accompanied with changes in cell fate and the direction of cell division similar to those observed upon polar transport inhibition (Figures 4E and 4F). Former endodermal cells expressed QC markers (Figure 4E). Adjacent cortex cells expressed the columella initial marker J2341 (data not shown) and divided (Figure 4F, arrowheads), and their daughters expressed columella markers (Figure 4F).

The respecification events that occurred upon addition of a large range of 2,4D concentrations (10^{-4} to 10^{-7} M) were similar, whereas 10^{-8} M induced neither DR5 staining nor respecification, suggesting that a range of internal concentrations provoke a similar response. Thus, absolute auxin levels and the slope of concentration differences are not sufficient to determine pattern and polarity, and additional positional cues are required. These cues may be in the form of a tissue prepattern, reflecting differences in the competence to respond to auxin, or they may originate from tissue(s) surrounding the responding cells.

To distinguish between tissue prepatterning and external cues, we performed laser ablations of the complete QC, which lead to complete respecification of the distal root cap and QC from distal vascular tissue (van den Berg et al., 1995). QC ablation resulted in a new DR5 peak in the distal vascular region within 2 days after ablation (Figures 5A and 5B). The appearance of

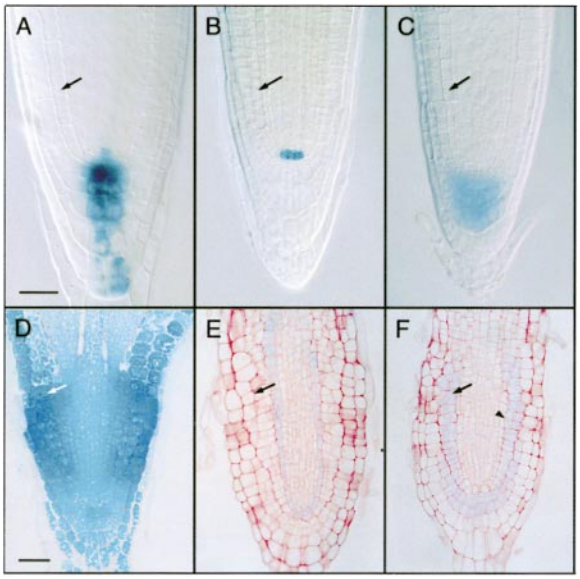

Figure 4. Exogenous Auxin Application Respecifies Distal Cell Fates in the Root Meristem

(A–C) 4 dpg seedlings, medium without auxin, DIC optics of cleared roots after GUS staining.
(D–F) 4 days after treatment of 2 dpg seedlings with 1 μM 2,4D. Ruthenium red–stained sections of GUS-stained root tips.
(A and D) *DR5/DR5*. (B and E) QC46/+. (C and F) A line heterozygous for the columella-specific promoter trap COL93.
Arrows indicate the position of cortex cell files. The arrowhead indicates a division in the former cortex. Bars, 25 μm.

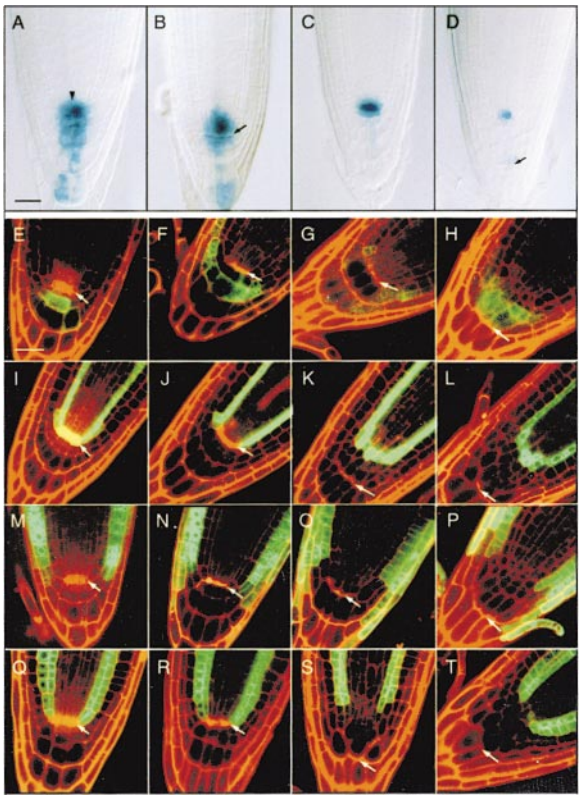

Figure 5. Regeneration of Distal Pattern Elements from Vascular Cells after Laser Ablation Occurs without Evidence for Transient Acquisition of Epidermal or Ground Tissue Fates

(A and B) Effect of QC ablation on the DR5 peak. DIC optics of cleared roots after GUS staining. (A) 5 dpg *DR5/DR5* seedling. Arrowhead: QC. (B) *DR5/DR5* seedling, 2 days after QC ablation at 3 dpg.
(C and D) Respecification of QC cells after QC ablation. (C) 7 dpg QC25/+ seedlings. (D) QC25/+ seedlings 4 days after QC ablation at 3 dpg.
(E–T) Expression of GFP-based markers after QC ablation. Superimposition of confocal images showing GFP distribution (green) and cell outlines stained by propidium iodide (red). Dead cells are bright red because of PI uptake, and yellow if they contain GFP prior to ablation.
(E–H) Columella-specific enhancer trap Q1630.
(I–L) *SCARECROW* promoter::GFP fusion.
(M–P) Epidermis-specific enhancer trap J2301.
(Q–T) Ground tissue (cortex/endodermis)–specific enhancer trap J0571.
(E, I, M, and Q) Immediately after ablation of 3 dpg plants. (F, J, N, and R) 1 day after ablation of the same plants; (G, K, O, and S) 3 days after ablation; (H, L, P, and T) 5 days after ablation.
Arrows indicate the position of the ablated QC. Bars, 25 μm.

this new DR5 peak and subsequent repatterning was dependent on polar auxin transport, because treatment with 0.5 μM NPA, which does not provoke the responses described in previous paragraphs, interfered with its establishment and with the respecification process. Columella and QC markers appeared in the respecified region 24 hr or more after the DR5 peak (Figures 5E–5H, 5C, and 5D). The position of the new QC, marked by expression of the QC25 marker (Figure 5D), was preceeded by expression of the *SCARECROW (SCR)* gene (Di Laurenzio et al., 1996) (Figures 5I–5L). *SCR* is expressed in the QC, but also in the cortical/endodermal initials and in the maturing endodermis. We tested whether the respecification events are the result of two sequential processes. A new ground tissue/protoderm prepattern could be established first, and these cells could subsequently be specified as distal cells by the perception of a new auxin maximum. However, the enhancer traps J2301 and J0571, which mark from embryogenesis onward respectively the entire root epidermis and cortex/endodermis, did not appear in the distal vascular region after QC ablation at any time during respecification (Figures 5M–5P and 5Q–5T). These data suggest that the *SCR* expression in the vascular region presaged QC respecification only, and that vascular cells are able to adopt QC and columella fate without transiently acquiring ground tissue or protoderm characteristics.

Our laser ablation experiments are not consistent with a predominant role for tissue prepattern in specifying distal cell types. The respecified QC and columella cells upon laser ablation are arranged in relation to their boundary with vascular cells, which is also the case upon NPA and auxin treatment. Therefore, information from vascular cells may be required to orient auxin responses in the distal root tip.

Discussion

Auxin Distribution Organizes Pattern

In this report we demonstrate that the *DR5::GUS* auxin response reporter displays maximum activity in distal cells of the *Arabidopsis* root tip. The response of this

maximum to external auxin and polar transport inhibitors, as well as measurements of free auxin contents are consistent with the notion that this reporter visualizes a distal auxin maximum, although at present we cannot independently measure auxin at cellular resolution. Mutants defective in auxin responses display decreased *DR5::GUS* activity, and correlated defects in distal cell specification. Mutants in auxin efflux carriers disturb the precise cellular localization of the maximum and display defects in patterned cell division and elongation. Our mutant analysis thus suggests that correct perception and localization of an auxin maximum are necessary for patterning. Ectopic auxin accumulation by three methods is sufficient to induce distal pattern and polarity in relation to the vascular bundle, indicating that high levels of auxin establish an "organizer" that specifies distal pattern elements in the *Arabidopsis* root meristem. Manipulation of multiple auxin transporters, i.e., in mosaic analyses, will be required to test this model.

Our evidence for the presence of a distal organizer and its relation to an asymmetric auxin distribution suggests a conceptual framework for diverse effects of auxins on tissue culture, embryo and root development (e.g., Skoog and Miller, 1957; Hadfi et al., 1998). If patterning relies on asymmetry through directional transport, a maximum resulting from initially coarse differences may specify cell types, as well as polarity and hence a new polar distribution of transporters. A system where transport influences fate and polarity, and vice versa, can have self-organizing properties that explain the flexibility of normal plant organogenesis and of atypical developmental processes such as tissue culture.

Below, we will discuss two questions raised by models where the asymmetric distribution of a single molecule, auxin, triggers the formation of a complex pattern. The first is how competence and prepattern affect the observed responses to auxin. The second is whether pattern elements are directly specified by differences in auxin abundance, or whether auxin acts as a switch to elicit a cascade of secondary events.

Competence and Prepattern in the Root

As auxin has been linked to a variety of patterning processes (Berleth and Jurgens, 1993; Przemeck et al., 1996; Hadfi et al., 1998; Hamann et al., 1999; Mattsson et al., 1999), it is important to determine which cells are competent to respond to auxins and whether spatial differences in competence (prepatterning information) determine the outcome of the response.

In the root, the meristem responds to auxin accumulation by respecification of distal pattern elements. Most maturing cells of the root do not respond, indicating that cell differentiation is accompanied by a loss of competence. The pericycle, however, responds to auxin addition by forming lateral roots. We note that lateral root formation during normal root development is also accompanied by DR5 promoter activity (our unpublished data), requires auxin (Kelly and Bradford, 1986; Celenza et al., 1995; Hobbie and Estelle, 1995), and involves specification of distal elements. Therefore, the different responses in the primary meristem and pericycle may result from similar organizer activities induced by an ectopic auxin maximum.

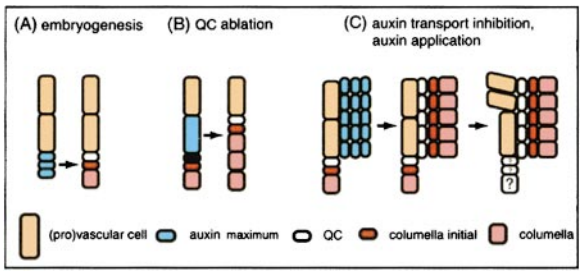

Figure 6. Model for the Organization of Distal Pattern by an Auxin Maximum in Relation to the Vascular Bundle

(A) During embryogenesis, the auxin maximum resides at the distal boundary of the provascular domain in the prospective QC and columella cells. (B) After QC ablation, a new distal auxin maximum is established in adjacent provascular cells, which are respecified as QC and columella with the original axis of polarity. (C) A lateral auxin maximum through auxin transport inhibition and auxin application leads to QC and columella specification from former endodermal and cortical cells. The polar axis is reoriented with respect to the provascular boundary.

Three distinct auxin distributions each specify pattern and polarity in the distal root tip in relation to the location of the vascular bundle (Figure 6). In the polar auxin transport inhibition and auxin application experiments, protodermal or ground tissue cells take on columella and QC identities. In the laser ablation experiments, vascular cells take on columella and QC identities without evidence for a transient switch to ground tissue or protoderm identities. Therefore, cells of all three major tissues are competent to form QC and columella cell types in response to high levels of auxin. The relation of newly specified distal cell types to the vascular bundle suggests that cell groups with peak auxin levels orient their axis of polarity toward the vascular bundle/pericycle (Figure 6). Emerging lateral roots show a similar relation between orientation of their polar axis and position of the auxin maximum.

Is Auxin a Morphogen?

In the mirror-image duplications, many features of pattern and polarity are changed in relation to a new auxin distribution, including cell fates, cell division planes, zones of mitotic activity, zones of cell elongation/differentiation, and polarity of epidermal root hair cells. Could an auxin concentration gradient directly specify these different features, or could auxin act to establish an organizer by triggering multiple short-range signaling events? In animal development, an original asymmetry may be translated into a final pattern with multiple cell states by direct concentration-dependent long-range action of the initial molecule—in this case called a morphogen—or by a short-range signal relay. Proving the case for a morphogen relies on showing that a factor forms a concentration gradient, and that it acts directly at a distance on responding cells in a concentration-dependent manner (for a discussion, see Neumann and Cohen, 1997).

Although direct measurements on tissue regions are not inconsistent with the existence of an auxin gradient in the root, reporters like *DR5::GUS* are only activated above a threshold, precluding detection of a gradient at

the cellular level. It is also not yet possible to distinguish between direct and indirect action of auxin at different distances of the localized maximum. Convincing evidence for direct action, in analogy with cases in *Drosophila*, requires cell-autonomous activation and repression of signal transduction and the availability of relevant direct downstream targets of signal transduction (Lecuit et al., 1996; Nellen et al., 1996). Our limited knowledge of the auxin signaling process currently precludes precise experiments, so the term "morphogen" for auxins seems preliminary. It is conceivable that some effects, like the reorientation of cell elongation, are directly mediated by auxin whereas others, like cell specification, do not directly depend on intracellular auxin concentration but result from threshold-dependent activation of secondary responses. The dissection of such downstream organizing events will be a future challenge.

Experimental Procedures

Materials and Growth Conditions

Arabidopsis thaliana mutants *axr1-3, axr1-12, pin1-1, eir1-1,* and *aux1-7* were obtained from the AIMS Seed Stock Center; *axr3-1* in ecotype Col-0 from O. L.; and mp^{U21} from Thomas Berleth. GUS-expressing promoter traps were selected from the INRA T-DNA lines (Bechtold et al., 1993). Enhancer traps lines J1092, J2301, J2341, J2672, and Q1630 are described in http://www.plantsci.cam.ac.uk/Haseloff/IndexCatalogue.html, and were kindly provided by Jim Haseloff. J0571 was obtained through the Nottingham stock center (N9094). p*SCR*::GFP and the LRC244 enhancer trap were constructed as described in Malamy and Benfey (1997a, 1997b). Construction of DR5::GUS is described in Ulmasov et al. (1997b). DR5::GUS homozygous plants were used to pollinate auxin mutants; mutants were selected in the F_2 and analyzed.

Seeds were sterilized in 5% sodium hypochloride, imbibed at 4°C in the dark in sterile water containing 0.1% agarose for 2–5 days, and germinated on plates containing 0.5× Murashige and Skoog (MS) salt mixture, 1% sucrose, and 0.5 g/l 2-(N-morpholino) ethanesulfonic acid (MES) pH 5.8, in 0.8% agar. Plates were incubated in a near vertical position at 22°C, 70% humidity and a cycle of 16 hr light/8 hr dark. Starch granules and β-glucoronidase activity were visualized as described (Willemsen et al., 1998).

Polar Auxin Transport Inhibition

In auxin transport inhibition experiments, the medium was supplemented with 10 or 50 μM NPA (Tokyo Kasei Kogyo Co., Ltd., Tokyo, Japan) or 30 μM TIBA (Sigma).

For the NPA and auxin treatments, five independent columella-specific markers have been used (Q1630, J2341, COL93, COL148, starch granule staining), four independent QC markers (QC46, QC25, QC142, QC184), two lateral root cap markers (J1092, LRC244), and two endodermis-specific (J2672, SCR::GFP) giving similar results in each case. When promoter traps were used, heterozygous plants were analyzed to avoid changes in phenotype due to gene disruption.

Exogenous Auxin Application

In exogenous applied auxin experiments, sterilized seeds were plated and grown as above and 2 dpg transferred to medium containing 10^{-8}–10^{-4} M 2,4-dichlorophenoxy acetic acid (2,4-D) (Duchefa, The Netherlands). Heterozygous promoter trap plants were analyzed.

Laser Ablations

Laser ablation experiments were performed using a Leica inverted confocal microscope and the Leica TCSNT software on 3 dpg seedlings as previously described (van den Berg et al., 1995).

Microscopy

Seedlings were embedded in Technovit 7100 (Kulzer, Hereaus), sectioned and stained with ruthenium red as described before (Scheres et al., 1994), and photographed on a Zeiss Axioskop microscope using Kodak Ektar 25 film. Embryos were dissected from ovules and stained for GUS activity as described (Willemsen et al., 1998). For light microscopy, plant material was cleared and mounted according to Scheres et al., 1994 and photographed using DIC optics on a Zeiss optiphot II microscope and Kodak Ektar 25 film.

Image Processing

Adobe PhotoShop V (Adobe Systems Inc., Mountain View, CA, USA) was used to assemble scanned photograph negatives and CSLM files.

Acknowledgments

We thank Frits Kindt, Ronald Leito, Piet Brouwer, and Wil Veenendaal for photography and assistance with Adobe PhotoShop; Jim Haseloff for generously making available GFP marker lines; Laurent Nussaume and Viola Willemsen for screening the Versailles T-DNA insertion collection; and NASC and AIMS for seed stocks. We are indebted to Goran Sandberg for sharing unpublished data and to Thomas Berleth for valuable discussions. S. S. is sponsored by a SON-NWO grant, D. B. holds an IKY grant and H. W. was supported by HFSPO grant RG 327/95.

Received August 16, 1999; revised October 26, 1999.

References

Bechtold, N., Ellis, J., and Pelletier, G. (1993). *In planta Agrobacterium* mediated gene transfer by infiltration of adult *Arabidopsis* plants. C. R. Acad. Sci. (Paris) *316*, 1194–1199.

Bennett, M.J., Marchant, A., Green, H.G., May, S.T., Ward, S.P., Millner, P.A., Walker, A.R., Schulz, B., and Feldmann K.A. (1996). *Arabidopsis AUX1* gene: a permease-like regulator of root gravitropism. Science *273*, 948–950.

Berleth, T., and Jurgens, G. (1993). The role of the *monopteros* gene in organising the basal body region of the *Arabidopsis* embryo. Development *118*, 575–587.

Celenza, J., Jr., Griafi, P., and Fink, G. (1995). A pathway for lateral root formation in *Arabidopsis thaliana*. Genes Dev. *9*, 2131–2142.

Chen, R., Hilson, P., Sedbrook, J., Rosen, E., Caspar, T., and Masson, P.H. (1998). The *Arabidopsis thaliana AGRAVITROPIC1* gene encodes a component of the polar-auxin-transport efflux carrier. Proc. Natl. Acad. Sci. USA *95*, 15112–15117.

Clark, S.E., Williams, R.W., and Meyerowitz, E.M. (1997). The *CLAVATA1* gene encodes a putative receptor kinase that controls shoot and floral meristem size in *Arabidopsis*. Cell *89*, 575–585.

Davies, P.J. (1995). Plant Hormones (Dordrecht, The Netherlands: Kluwer Academic Publishers).

Delbarre, A., Muller, P., Imhoff, V., and Guern, J. (1996). Comparison of mechanisms controlling uptake and accumulation of 2,4-dichlorophenoxy acetic acid, naphthalene-1-acetic acid, and indole-3-acetic acid in suspension-cultured tobacco cells. Planta *198*, 532–541.

Di Laurenzio, L., Wysockadiller, J., Malamy, J., Pysh, E., Helariutta, Y., Freshour, G., Hahn, M.G., Feldmann, K.A., and Benfey, P.N. (1996). The *SCARECROW* gene regulates an asymmetric cell division that is essential for generating the radial organization of the *Arabidopsis* root. Cell *86*, 423–433.

Dolan, L., Janmaat, K., Willemsen, V., Linstead, P., Poethig, S., Roberts, K., and Scheres, B. (1993). Cellular organisation of the *Arabidopsis* root. Development *119*, 71–84.

Fletcher, J.C., Brand, U., Running, M.P., Simon, R., and Meyerowitz, E.M. (1999). Signaling of cell fate decisions by *CLAVATA3* in *Arabidopsis* shoot meristems. Science *283*, 1911–1914.

Galweiler, L., Guan, C., Muller, A., Wisman, E., Mendgen, K., Yephremov, A., and Palme, K. (1998). Regulation of polar auxin transport by *AtPIN1* in *Arabidopsis* vascular tissue. Science *18*, 2226–2230.

Hadfi, K., Speth, V., and Neuhaus, G. (1998). Auxin-induced developmental patterns in *Brassica juncea* embryos. Development *125*, 879–887.

Hamann, T., Mayer, U., and Jurgens, G. (1999). The auxin-insensitive *bodenlos* mutation affects primary root formation and apical-basal patterning in the *Arabidopsis* embryo. Development *126*, 1387–1395.

Hardtke, C.S., and Berleth, T. (1998). The *Arabidopsis* gene *MONOPTEROS* encodes a transcription factor mediating embryo axis formation and vascular development. EMBO J. *17*, 1405–1411.

Hobbie, L., and Estelle, M. (1995). The *axr4* auxin-resistant mutants of *Arabidopsis thaliana* define a gene important for root gravitropism and lateral root initiation. Plant J. *7*, 211–220.

Ingham, P.W., and Martinez Arias, A. (1992). Boundaries and fields in early embryos. Cell *68*, 221–235.

Kelly, M.O., and Bradford, K.J. (1986). Insensitivity of the *diageotropica* tomato mutant to auxin. Plant Physiol. *82*, 713–717.

Kim, J., Harter, K., and Theologis, A. (1997). Protein-protein interactions among the Aux/IAA proteins. Proc. Natl. Acad. Sci. USA *94*, 11786–11791.

Lecuit, T., Brook, W.J., Ng, M., Calleja, M., Sun, H., and Cohen, S.M. (1996). Two distinct mechanisms for long-range patterning by *Decapentaplegic* in the *Drosophila* wing. Nature *381*, 387–393.

Leyser, O., Lincoln, C.A., Timpte, C., Lammer, D., Turner, J., and Estelle, M. (1993). *Arabidopsis* auxin-resistance gene *AXR1* encodes a protein related to ubiquitin-activating enzyme E1. Nature *364*, 161–164.

Liu, C.-M., Xu, Z.-H., and Chua, N.-H. (1993). Auxin polar transport is essential for the establishment of bilateral symmetry during early plant embryogenesis. Plant Cell *5*, 621–630.

Luschnig, C., Gaxiola, R.A., Grisafi, P., and Fink, G.R. (1998). EIR1, a root-specific protein involved in auxin transport, is required for gravitropism in *Arabidopsis thaliana*. Genes Dev. *12*, 2175–2187.

Malamy, J.E., and Benfey, P.N. (1997a). Organization and cell differentiation in lateral roots of *Arabidopsis thaliana*. Development *124*, 33–44.

Malamy, J.E., and Benfey, P.N. (1997b). Analysis of *SCARECROW* expression using a rapid system for assessing transgene expression in *Arabidopsis* roots. Plant J. *12*, 957–963.

Marchant, A., Kargul, J., May, S.T., Muller, P., Delbarre, A., Perrot-Rechenmann, C., and Bennett, M.J. (1999). *AUX1* regulates root gravitropism in *Arabidopsis* by facilitating auxin uptake within root apical tissues. EMBO J. *18*, 2066–2073.

Mattsson, J., Sung, Z.R., and Berleth, T. (1999). Responses of plant vascular systems to auxin transport inhibition. Development *126*, 2979–2991.

Muller, A., Guan, C., Galweiler, L., Tanzler, P., Huijser, P., Marchant, A., Parry, G., Bennett, M., Wisman, E., and Palme, K. (1998). *AtPIN2* defines a locus of *Arabidopsis* for root gravitropism control. EMBO J. *17*, 6903–6911.

Nellen, D., Burke, R., Struhl, G., and Basler, K. (1996). Direct and long-range action of a *Dpp* morphogen gradient. Cell *85*, 357–368.

Neumann, C.J., and Cohen, S. (1997). Morphogens and pattern formation. BioEssays *19*, 721–729.

Parcy, F., Nilsson, O., Busch, M.A., Lee, I., and Weigel, D. (1998). A genetic framework for floral patterning. Nature *395*, 561–566.

Przemeck, G.K., Mattsson, J., Hardtke, C.S., Sung, Z.R., and Berleth, T. (1996). Studies on the role of the Arabidopsis gene *MONOPTEROS* in vascular development and plant cell axialization. Planta *200*, 229–237.

Rouse, D., Mackay, P., Stirnberg, P., Estelle, M., and Leyser, O. (1998). Changes in auxin response from mutations in an *AUX/IAA* gene. Science *279*, 1371–1373.

Rubery, H.P. (1990). Phytotropins: receptors and endogenous ligands. Symp. Soc. Exp. Biol. *44*, 119–146.

Ruegger, M., Dewey, E., Gray, W.M., Hobbie, L., Turner, J., and Estelle, M. (1998). The TIR1 protein of *Arabidopsis* functions in auxin response and is related to human SKP2 and yeast grr1p. Genes Dev. *12*, 198–207.

Sachs, T. (1991). Cell polarity and tissue patterning in plants. Development (Suppl.) *1*, 83–93.

Scheres, B., Wolkenfelt, H., Willemsen, V., Terlouw, M., Lawson, E., Dean, C., and Weisbeek, P. (1994). Embryonic origin of the *Arabidopsis* primary root and root meristem initials. Development *120*, 2475–2487.

Sessions, A., Nemhauser, J.L., McColl, A., Roe, J.L., Feldmann, K.A., and Zambryski, P.C. (1997). *ETTIN* patterns the *Arabidopsis* floral meristem and reproductive organs. Development *124*, 4481–4491.

Skoog, F., and Miller, C.O. (1957). Chemical regulation of growth and organ formation in plant tissues cultured *in vitro.* Symp. Soc. Exp. Biol. *11*, 118–131.

Steeves, T.A., and Sussex, I.M. (1989). Patterns in Plant Development (Cambridge: Cambridge University Press).

St. Johnston, D., and Nusslein-Volhard, C. (1992). The origin of pattern and polarity in the *Drosophila* embryo. Cell *68*, 201–219.

Tian, Q., and Reed, J.W. (1999). Control of auxin-regulated root development by the *Arabidopsis SHY2/IAA3* gene. Development *126*, 711–721.

Uggla, C., Moritz, T., Sandberg, G., and Sundberg, B. (1996). Auxin as a positional signal in pattern formation in plants. Proc. Natl. Acad. Sci. USA *93*, 9282–9286.

Ulmasov, T., Hagen, G., and Guilfoyle, T.J. (1997a). *ARF1*, a transcription factor that binds to auxin response elements. Science *276*, 1865–1868.

Ulmasov, T., Murfett, J., Hagen, G., and Guilfoyle, T.J. (1997b). Aux/IAA proteins repress expression of reporter genes containing natural and highly active synthetic auxin response elements. Plant Cell *9*, 1963–1971.

Ulmasov, T., Hagen, T., and Guilfoyle, T.J. (1999). Activation and repression of transcription by auxin-response factors. Proc. Natl. Acad. Sci. USA *96*, 5844–5849.

van den Berg, C., Willemsen, V., Hage, W., Weisbeek, P., and Scheres, B. (1995). Cell fate in the *Arabidopsis* root meristem determined by directional signaling. Nature *378*, 62–65.

van den Berg, C., Willemsen, V., Hendriks, G., Weisbeek, P., and Scheres, B. (1997). Short-range control of cell differentiation in the *Arabidopsis* root meristem. Nature *390*, 287–289.

Walker, L., and Estelle, M. (1998). Molecular mechanisms of auxin action. Curr. Opin. Plant Biol. *1*, 434–439.

Willemsen, V., Wolkenfelt, H., de Vrieze, G., Weisbeek, P., and Scheres, B. (1998). The *HOBBIT* gene is required for formation of the root meristem in the *Arabidopsis* embryo. Development *125*, 521–531.